An Integrated Study of Small-Angle X-ray Scattering and Dynamic Light Scattering on Cylindrical Micelles of Sodium Glycodeoxycholate

Luciano Galantini,* Edoardo Giglio, Antonio Leonelli, and Nicolae Viorel Pavel

Dipartimento di Chimica, Università di Roma "La Sapienza", P.le A. Moro 5, 00185 Roma, Italy

Received: September 15, 2003; In Final Form: December 5, 2003

Small-angle X-ray scattering (SAXS) and dynamic light scattering (DLS) measurements were carried out on aqueous micellar solutions of the ionic biological detergent sodium glycodeoxycholate (NaGDC). Apparent diffusion coefficients (D_{app}) and SAXS spectra of NaGDC 0.1 M solutions at different ionic strengths (0−0.4 M NaCl added) were reported. Moreover, a D_{app} study as a function of NaGDC concentration c (20−60 mM) in the range 0−0.3 M NaCl was performed. A drastic change of the D_{app} versus c slope indicates that as the electrolyte concentration is increased, the effect of the repulsive electric double layer is lowered, until a dominance of the van der Waals attraction effect is evidenced at the highest ionic strengths. A comparative analysis of SAXS spectra and D_{app} data confirms this result. A uniform cylinder was used to model the micelle in the data interpretation. The effect of interactions on SAXS spectra was explored in terms of the decoupling approximation. Restricted to the NaCl concentrations where the Coulombic repulsions predominate, the method of Hayter and Penfold for a charged hard sphere system was used to compute the interparticle structure factor $S(q)$. To compare SAXS and DLS data in the same range, a solution of hard cylinders with larger effective dimensions was also used to represent the micelle samples, thus allowing the determination of the hydrodynamic radii. By increasing the NaCl concentration from 0 to 0.2 M, an almost constant micellar diameter of 32−34 Å and a growing micellar length from 38 to 64 Å were obtained. At the same time, increasing hydrodynamic radii from 16 to 26 Å were estimated.

Introduction

The physical chemistry of colloids represents a very interesting research topic both from a biological and technological point of view. Among the methods available to study systems containing colloidal particles, those based on the measurements of scattering and transport properties have proved to be very useful. The data analysis for all these techniques is relatively easy for dilute and monodisperse particle solutions. In fact, at the limit of infinite dilution these data depend only on the geometry of the individual particles. On the other hand, for more concentrated systems, the data interpretation becomes much more complicated because of interparticle correlation. This phenomenon is related to the particle interaction potential and is enhanced in solutions of charged particles because of the strong electrostatic component in the interaction potential. In this case, moreover, the interpretation of the transport properties is complicated by the interactions between colloidal particles and other ionic species (counterions, added salt ions, etc.). Several studies are reported in the literature where the electrostatic coupling between all the ionic species in charged colloidal particle solutions is considered to rationalize the experimental diffusion coefficient behavior. The concentration dependence of experimental diffusion coefficients is interpreted, in these cases, in terms of a weak colloidal electrolyte diffusion.[1−5]

Normally, information on size and shape of colloidal particles are extracted by extrapolating to infinite dilution the experimental data. However, this extrapolation is impossible if self-assembling systems with concentration dependent aggregation number are studied. Ionic micelle solutions well represent this kind of system since these micelles grow by varying either amphiphile concentration or ionic strength. Hence, the influence of particle correlation on diffusivity and scattering must be quantified to treat these colloidal systems. Several approximated expressions are available in the literature to this aim. However, knowledge of the particle interaction potential is crucial to apply these expressions to real systems. In solutions of interacting Brownian particles, two types of interactions can be identified. These are hydrodynamic interactions, transmitted by the solvent flow and depending on the friction matrix coefficients, and direct interactions. According to the standard DLVO theory[6] of colloidal stability, the direct interaction potential between two ionic micelles is generally expressed as the sum of three independent parts: (i) a hard-body repulsion representing the excluded-volume effect of the micelles, (ii) an electric double layer repulsion between two micelles surrounded by their own ionic atmosphere, and (iii) a long-range van der Waals attraction.

A particular class of ionic amphiphiles is constituted by bile salts. These compounds are extremely important biological surfactants, mainly because of their ability to solubilize and carry a wide variety of molecules in aqueous physiological solutions.[7,8] Dynamic light scattering (DLS) results on bile salt and other ionic surfactant micelles show that their diffusivities vary by changing both the amphiphile concentration and the ionic strength.[9−23] Both particle interaction effect and micellar size variation give rise to the diffusion coefficient experimental trends. At low NaCl concentration, because of the repulsive electrostatic interactions,[11,17−20] particle correlation appears to be the most important factor influencing the DLS measurements. Models based exclusively on intermicellar interactions were proposed to explain the data in these conditions and allowed

* Corresponding author. Telephone: (+39)-6-49913687; fax: (+39)-6-490631; e-mail: l.galantini@caspur.it.

10.1021/jp036746b CCC: $27.50
Published on Web 02/06/2004

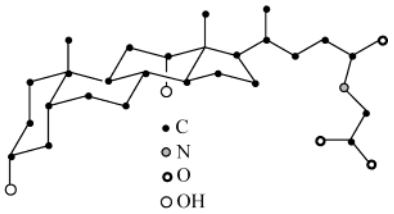

Figure 1. Molecular formula of the glycodeoxycholate anion.

the definition of the DLVO interaction potential.[17−20] A study based on this kind of models has been recently accomplished on micellar solutions of a bile salt by Janich et al.[11] Solutions of sodium glycodeoxycholate (NaGDC) (Figure 1) with added NaCl were analyzed. Both apparent molar mass and apparent diffusion coefficient (D_{app}) were determined by means of static light scattering and DLS measurements. In the dilute region, they found that both the quantities vary monotonically by increasing the bile salt concentration. From the slope of these trends, the authors suggest that a progressive screening of the DLVO potential electrostatic component is induced by increasing the ionic strength. To extract information on particle interactions, it was supposed that, at low NaCl molarity ($\leq$0.2 M), NaGDC micelle size does not depend on the bile salt concentration. Under this assumption, they could determine the parameters of DLVO intermicellar potential by fitting the D_{app} and the molar mass concentration dependences. Both the hydrodynamic radii and the molar mass were shown to grow by increasing the NaCl concentration. Published results indicate that NaGDC, as well as other bile salts with similar amphiphile properties (sodium taurodeoxycholate and deoxycholate), give rise to rod shape micelles because of the growth process.[12,13,24]

Starting from these basic findings, small-angle X-ray scattering (SAXS) and DLS measurements on NaGDC micellar solutions at different NaCl concentrations have been integrated in this paper. A homogeneous hard cylinder was considered to represent the micelle in the experimental data interpretation. The decoupling approximation was used to evaluate the effect of interactions on SAXS spectra.[25] First, a comparison of the two techniques measurements was performed, by assuming an interaction potential constituted by the hard-body component alone, to investigate the character of the intermicellar interactions at different ionic strengths. Afterward, restricted to the samples at low ionic strength, the SAXS spectra were fitted by using the mean spherical approximation (MSA), as developed by Hayter and Penfold, to estimate the effect of electrostatic repulsions on the interparticle structure factor $S(q)$.[26,27] Moreover, to compare SAXS and DLS data, an interpretation model constituted by a solution of cylinders with a suitable hard interaction shell was also used to represent the micelle samples in these conditions.[28] The hydrodynamic radii were obtained in this way without extrapolating at infinite dilution the micelle D_{app} values.

Theoretical Background

DLS Data Treatment. In general, a dynamic particle solution gives rise to a time-varying scattered intensity because of the particle Brownian motion. In a DLS experiment, the temporal fluctuations of the scattered intensity are analyzed by estimating the normalized intensity−intensity time autocorrelation function that, at the scattering vector q, is defined as

$$g_2(q,\tau) = \frac{\langle I(q,0)I(q,\tau)\rangle}{\langle I(q)\rangle^2}$$

For a Gaussian distribution of the intensity profile, $g_2(q,\tau)$ is related to the normalized field autocorrelation function $g_1(q,\tau)$ as[29,30]

$$g_2(q,\tau) = 1 + B|g_1(q,\tau)|^2$$

In the most general cases, $g_1(q,\tau)$ is analyzed through the cumulant expansion and the apparent diffusion coefficient D_{app} is obtained from the first cumulant by the relation

$$D_{app} = -\frac{1}{q^2}\frac{d \ln g_1(q,\tau)}{d\tau}\Big|_{\tau=0}$$

In the hydrodynamic limit, $g_1(q,\tau)$ describes the spatial fluctuations of particle concentrations.[31] In the simplest case of monodisperse particles, $g_1(q,\tau)$ decays as a single exponential and D_{app} is equal to the collective diffusion coefficient. Moreover, because of particle interaction, D_{app} is concentration dependent and to a first order we have

$$D_{app} = D_o(1 + \lambda_c\phi) \tag{1}$$

where ϕ is the diffusing particle volume fraction, and the diffusion coefficient at infinite dilution is given by

$$D_o = \frac{kT}{6\pi\eta R_h} \tag{2}$$

with k, T, R_h, and η representing the Boltzmann constant, the absolute temperature, the hydrodynamic radius of the diffusing particles, and the medium viscosity, respectively.

The parameter λ_c is often called the diffusion second virial coefficient and is generally expressed as

$$\lambda_c = (\lambda_V - 1 - \lambda_f) \tag{3}$$

where λ_f is the linear term coefficient in the expansion of the friction factor in powers of volume fraction and λ_V is linked to the thermodynamic second virial coefficient.[28,32] For a system of hard-body interacting rigid rods with a length L and a diameter d we have from the theory developed by Ishihara[33]

$$\lambda_V = \frac{\pi N_A d^2 L}{2\bar{V}}\left[\frac{L}{d} + \frac{1}{2}(3+\pi) + \frac{\pi}{4}\frac{d}{L}\right] \tag{4}$$

Moreover, according with an expression derived by Peterson,[34] λ_f can be expressed as

$$\lambda_f = \frac{kN_A T L^2}{3\eta D_o \bar{V}}\left(\frac{3d}{8L}\right)^{2/3} \tag{5}$$

with $\bar{V}$ and N_A representing the cylindrical particle molar volume and Avogadro's number, respectively.

For rigid rods with $2 \leq L/d < 30$, Tirado and Garcia de la Torre give the following

$$D_o = \frac{kT\left(\ln\frac{L}{d} + \gamma\right)}{3\pi\eta L} \tag{6}$$

where $\gamma = 0.312 + 0.565d/L - 0.100d^2/L^2$.[35,36] If this expression is substituted in eq 5 and the cylinder molar volume $\bar{V} = \pi d^2 L N_A/4$ is assumed, the following equation which gives the dependence of λ_f on L/d only is obtained[37]

$$\lambda_f = 4\frac{L^2}{d^2}\left(\frac{3}{8}\frac{d}{L}\right)^{2/3}\left(\ln\left(\frac{L}{d}\right)+\gamma\right)^{-1} \quad (7)$$

and, by substituting eqs 4 and 7 in eq 3, we have

$$\lambda_c = 2\left[\frac{L}{d}+1+\frac{\pi}{2}+\frac{\pi}{4}\frac{d}{L}\right]-4\frac{L^2}{d^2}\left(\frac{3}{8}\frac{d}{L}\right)^{2/3}\left(\ln\left(\frac{L}{d}\right)+\gamma\right)^{-1} \quad (8)$$

as far as λ_c is concerned.

SAXS Data Treatment. A small-angle scattering experiment measures the intensity pattern of coherently scattered radiation that is constructed by the arrangement of scattering centers in solutions. The scattered intensity is reported as a function of the magnitude of the scattering vector q. A SAXS spectrum is reported in term of the differential scattering cross section per unit volume ($I(q)$) and is a function of the electron density distribution within the particles and of the particle distribution within the solution. The contribution of a single particle j to the total scattered intensity is generally expressed in terms of scattering form factor $F(q)$ defined as

$$F_j(q) = \int \Delta\rho \exp(iq\cdot r)dV_j$$

where $\Delta\rho$ is the difference between the j particle and the solvent electron density.

In the diluted solutions, particle interactions can be neglected and the form factor alone describes the scattered intensity. On the other hand, in a solution of interacting particles, correlation among the particle positions and orientations takes place. In this paper, the effects of particle interactions on scattering spectra are explored in terms of the decoupling approximation.[25] The basic assumption of this approximation is that particle orientations are not correlated to the positions. The final result of the treatment is that, for a solution of particles with N_p particle density, $I(q)$ can be expressed as

$$I(q) = N_p\langle|F(q)|^2\rangle\left[1+\frac{|\langle F(q)\rangle|^2}{\langle|F(q)|^2\rangle}(S(q)-1)\right] \quad (9)$$

where, as a function of the particle positions r_j, the interparticle structure factor is given by

$$S(q) = N_p^{-1}\left\langle\sum_{k=1}^{N_p}\sum_{j=1}^{N_p}\exp[iq\cdot(r_k-r_j)]\right\rangle$$

and, for systems of monodisperse particles, the angular brackets denote the average over all the orientations.

In practical applications, the determination of $S(q)$ needs the particles to be redefined as equivalent spheres. In the case of elongated particles, the radius of the equivalent sphere is determined by equating the second virial coefficient of the elongated particle to the second virial coefficient of a hard sphere solution. Generally, prolate ellipsoid of revolution is considered to represent the elongated particle. This method gave good results in the treatment of several spherocylindrical micelles.[25,38,39] However, the structural models reported in the literature indicate that, because of their peculiar amphiphilic structure (Figure 1), bile salts give rise to elongated micelles that are well approximated by cylinders. By considering the equivalence between second virial coefficients of cylinders and spheres, the equivalent diameter δ can be expressed as

$$\delta = \frac{1}{2}\left\{3d^2L\left[\frac{L}{d}+\frac{1}{2}(3+\pi)+\frac{\pi}{4}\frac{d}{L}\right]\right\}^{1/3} \quad (10)$$

A solution of hard spheres with an effective diameter expressed as in eq 10 can be considered to mimic the interparticle correlation in a system of hard cylinders. Hence, the interparticle structure factor can be determined by applying to this system the closed form to the Percus Yevick approximation. In the calculation, a micellar volume $v_m = \pi d^2L/4$ can be assumed, whereas the aggregation number n and the volume fraction ϕ_o can be estimated as

$$n = \frac{v_m}{v} \quad (11a)$$

$$\phi_o = \frac{\pi\delta^3 N_A(c-cmc)}{6n} \quad (11b)$$

where c and cmc are the NaGDC total and critical micelle molarity, respectively, and v represents the specific micellar volume per monomer.

On the other hand, the following form factor orientational averages must be used in eq 9

$$\langle|F(q)|^2\rangle = \int_0^{\pi/2}|F(q,L,d,\beta)|^2\sin\beta d\beta$$

$$|\langle F(q)\rangle|^2 = \left|\int_0^{\pi/2}F(q,L,d,\beta)\sin\beta d\beta\right|^2$$

Thus, for homogeneous cylinders we have[40]

$$F(q,L,d,\beta) = 2\pi d^2L\Delta\rho\frac{\sin\left(q\frac{L}{2}\cos\beta\right)J_1\left(q\frac{d}{2}\sin\beta\right)}{q^2Ld\sin\beta\cos\beta}$$

where $J_1(s)$ represents the first-order Bessel function of argument s and β is the orientation angle.

Experimental Section

Materials. NaGDC (Sigma) and NaCl (Merck, suprapur) were used.

DLS Measurements. Brookhaven instrument constituted by a BI-2030AT digital correlator with 136 channels and a BI-200SM goniometer was used. The light source was a Uniphase solid-state laser system model 4601 operating at 532 nm. Dust was eliminated by means of a Brookhaven ultrafiltration unit (BIUU1) for flow-through cells, the volume of the flow cell being about 1.0 cm^3. Nuclepore filters with a pore size of 0.1 μm were used. The samples were placed in the cell for at least 30 min prior to the measurement to allow for thermal equilibration. Their temperature was kept constant within 0.5 °C by a circulating water bath. The time-dependent light-scattering correlation function was analyzed only at the 90° scattering angle. Apparent diffusion coefficients did not depend on the exchanged wave vector in the range 30−150° in our experimental conditions.

SAXS Measurements. The measurements have been carried out in quartz capillary of 1 mm by using a Kratky compact system equipped with a NaI scintillation counter in a temperature-controlled room at 25 ± 1 °C. Ni-filtered Cu Kα radiation (λ = 1.5418 Å) was used. Scattering curves were recorded within the range $0.012 \le q \le 0.5$ Å^{-1} ($q = 4\pi\sin\theta/\lambda$). The moving slit method has been employed to measure the intensity of the primary beam and the scattering intensities have been put on an absolute scale.[41] In the minimization procedures, the calculated intensities have been smeared by the normalized weighting functions for slit length and slit width effects[42] and the best agreement with the experimental data has been obtained by minimizing the function

$$R = \frac{1}{N}\sum_{i=1}^{N}\frac{(Io_i(q) - Ic_i(q))^2}{\sigma_i^2}$$

where $Io_i(q)$ and $Ic_i(q)$ are the smeared observed and calculated intensities, σ_i^2 is the $Io_i(q)$ variance, and N is the number of experimental points.

Results and Discussion

Ionic Strength Effect on Micellar Interaction Potential. The D_{app} of NaGDC aqueous solutions as a function of NaGDC concentration at different ionic strength are reported in Figure 2. The obtained trends are in agreement with those of ref 6 and, accordingly with a common behavior of ionic micelles, their slope varies from positive to negative by increasing the NaCl concentration.

The D_{app} concentration dependence is affected by the λ_c value (eq 1) which is influenced by the nature of particle interactions. Generally, a simple hard-body interaction potential yields a positive λ_c. The repulsive electrostatic component of the potential increases the λ_c value, whereas the attractive part tends to reduce it and may lead, if large enough, to negative values. When $\lambda_c < 0$, attraction is more effective than repulsion. In view of these considerations, the observed results indicate that the repulsive electrostatic potential prevails on the attractive one in the NaGDC micellar solution at low ionic strength. By increasing the electrolyte concentration, the electrostatic interaction becomes more and more screened, and, beyond a critical point, the attractive potential prevails. Therefore, two distinct NaCl concentration ranges can be identified where attraction or electrostatic repulsion predominates. The results reported in ref 6 show that the micelles grow with increasing ionic strength. In the range where attraction prevails, a growth as a function of the bile salt concentration is also proposed.

Dynamic light scattering measurements were carried out also on NaGDC 0.1 M aqueous solutions at different NaCl concentration (Figure 3). A decrease of D_{app} by increasing the ionic strength is observed, probably because of both the micellar growth and the progressive screening of the electrostatic repulsions.

SAXS spectra were recorded on the same solutions of Figure 3 (Figure 4). Very different $I(q)$ profiles characterize repulsively or attractively interacting particle systems.[38,39] In agreement with the D_{app} trends (Figures 2 and 3), the $I(q)$ patterns of Figure 4 gradually lose the typical shape of repulsively interacting particle samples by increasing the NaCl concentration. At the same time, they show a relevant increase of the absolute scattered intensity at low q, thus testifying the micellar growth process.

As a first approach, we tried to fit all the SAXS spectra by assuming that, of the three contributions expected from the DLVO theory, the excluded-volume component alone represents the particle interaction potential, thus using the simple hard-body model described in the SAXS Data Treatment section. Variable length L, diameter d, specific volume per monomer υ, and $\Delta\rho$ were assumed to fit the experimental data. The $\Delta\rho$ value was chosen as the best scaling factor between calculated and experimental data. Despite the very different shape of the experimental spectra, we found that this model always provides satisfactory fits (Figure 4).

The best fitting L, d, and υ parameters are reported in Figure 5.

On the basis of the DLVO theory, the interaction model that we assumed in this preliminary analysis is realized when the attractive and the electrostatic repulsive component compensate each other. Of course, except for the samples where this condition is at least approximately verified, L, d, and υ in Figure 5 must be considered as fitting values only, since they lose their meaning of geometrical parameters of the micelles.

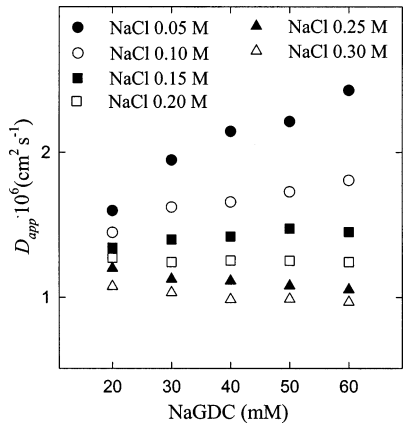

Figure 2. D_{app} of NaGDC aqueous solutions as a function of concentration at different ionic strengths and at 25 °C. Esd's are within 3%.

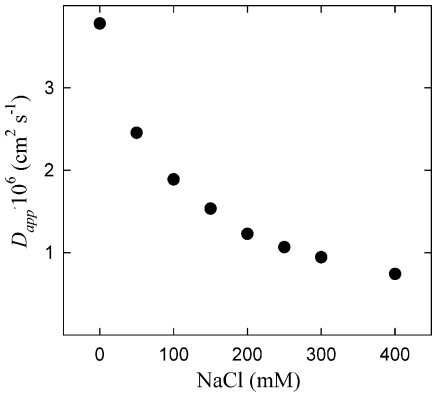

Figure 3. D_{app} values of 0.1 M NaGDC aqueous solutions as a function of NaCl concentrations at 25 °C. Esd's are within 0.5%.

A check on the reliability of the SAXS fitting parameters of Figure 5 was performed by involving the D_{app} data of Figure 3. In this procedure, we supposed that the same homogeneous cylinder well represents both X-ray scattering and hydrodynamic properties of the micelle. Under this hypothesis, the same micelle structure parameters should be able to interpret experimental SAXS spectra and D_{app} values, whenever a realistic interaction model is assumed. To analyze this condition, from the L and d values of Figure 5, D_o and λ_c were calculated by means of eqs 6 and 8, respectively. Hence, by means of eq 1, a specific micellar volume per monomer υ_D was inferred from the experimental D_{app} as follows

$$\upsilon_D = \frac{\phi}{N_A(c - cmc)} = \frac{D_{app} - D_o}{N_A D_o \lambda_c (c - cmc)}$$

As shown in Figure 5, different υ_D and υ values are generally obtained. However, the two curves of υ and υ_D as a function of the ionic strength cross at about 0.2 M NaCl concentration. In view of the previous statements, when different υ and υ_D values are obtained the parameters of Figure 5 must be considered as fitting variables only and do not really represent the micelle geometry, thus indicating that the adopted hard-body interaction model is unrealistic. On the other hand, the sample where the two values coincide represents the conditions where the attractive van der Waals contribution roughly compensates the

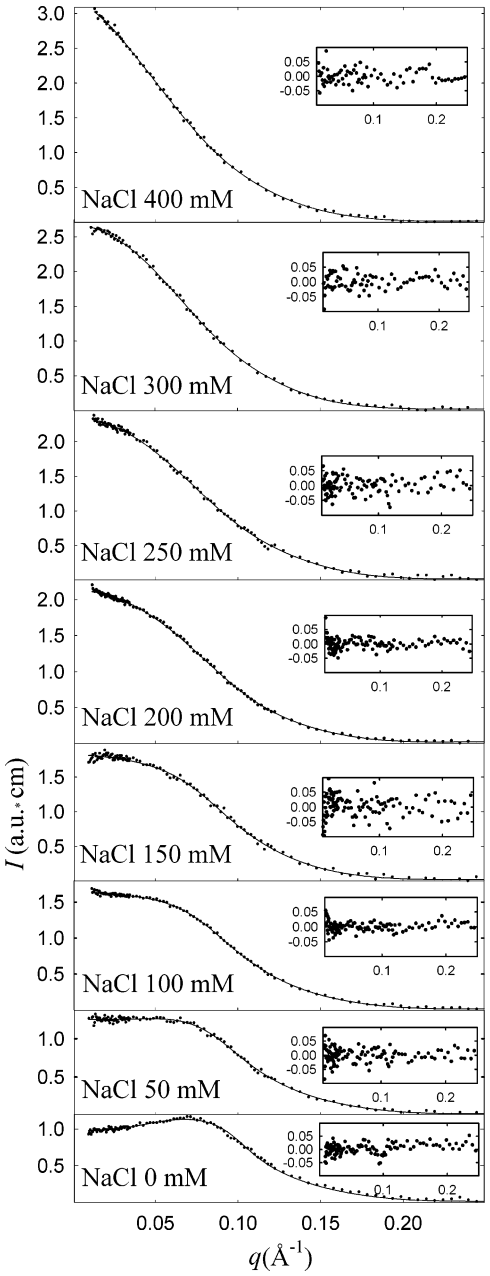

Figure 4. SAXS spectra of 0.1 M NaGDC micellar solutions at different NaCl concentrations and at 25 °C (dots). The solid lines are the theoretical fits on the basis of the model considering only the excluded-volume component of the particle interaction potential (see text). The residuals are reported in the inset.

repulsive electrostatic one and the hard-body component alone well approximates the micelle interaction potential. Hence, in this case v, L, and d preserve their physical meaning and can be considered reliable values of the micellar volume per monomer, length, and diameter of the cylindrical micelle, respectively. Reasonably, this condition is realized at the NaCl concentration which signs the crossover between the above-mentioned ranges where electrostatic repulsions or attractions predominate. This concentration cannot be inferred from the trends of Figure 2 if no restriction on the micellar growth is imposed. By assuming a micellar size invariance within the 20−60 mM NaGDC concentration range, a crossover NaCl concentration of 0.2 M was roughly pointed out in ref 6, in agreement with our results. At this electrolyte concentration $L = 64.0 \pm 0.8$ Å, $d = 34.0 \pm 0.4$ Å, $v = 900 \pm 15$ Å^3 (v_o), and

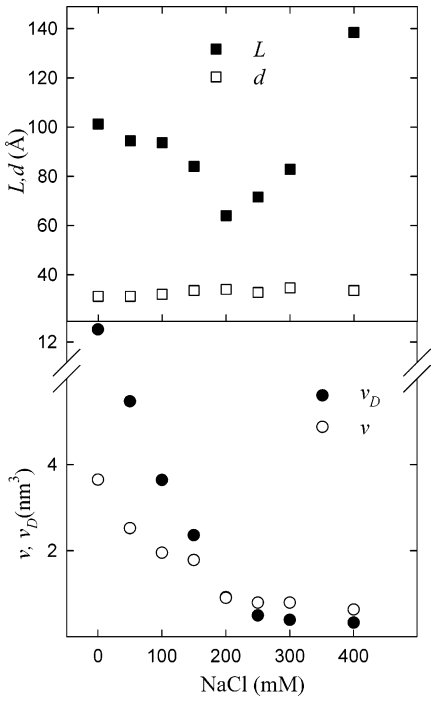

Figure 5. Fitting parameters of the calculated scattering intensities of Figure 4 as a function of NaCl concentration. In the lower panel, v_D values obtained by integrating SAXS fitting parameters and the D_{app} data are also reported (see text).

$\Delta\rho = 0.0363$ electrons Å^{-3} ($\Delta\rho_o$) are obtained. An aggregation number of 65 ± 4 is estimated from these parameters by means of eq 11.

As shown in Figure 4 $v_D > v$ and $v_D < v$ characterize the low and the high ionic strength ranges, respectively, whereas almost constant d values are obtained at all the NaCl concentrations. As far as L is concerned, a peculiar pattern with a minimum at the estimated crossover electrolyte concentration is observed. Obviously, the decreasing trend at NaCl concentration <0.2 M is unrealistic since it disagrees with the general behavior of NaGDC and other ionic surfactant micelles which normally grow by increasing the ionic strength. In fact, this result confirms that a relevant repulsive potential, which is not considered in this preliminary analysis, is present in the low electrolyte concentration range.

Measurement Interpretation at Low Ionic Strength. At the moment, no exhaustive method to estimate $S(q)$ for interaction potential with both significant attractive van der Waals and repulsive Debye Hückel component is available. However, for ionic micelle systems at very low or very high NaCl concentration, where the attractive or repulsive component is disregarded, respectively, a hard-body potential with a Yukawa tail can be used to describe the interaction potential, and the method of Hayter and Penfold, on the basis of the MSA,[26] is suitable to evaluate $S(q)$. This method was used in this work to fit the SAXS spectra at NaCl concentration ≤0.15 M. As is usually done when micellar solutions with low added electrolyte concentration are studied, we considered the micelle to be represented by a rigid equivalent sphere interacting through a screened electric double layer interaction potential (EDL interaction model) expressed as

$$U(r) = \frac{\alpha^2 n^2 e^2}{\pi\epsilon_o\epsilon r(2+\kappa\delta)^2}\exp[-\kappa(r-\delta)]$$

where r is the intermicellar center to center distance, ϵ is the

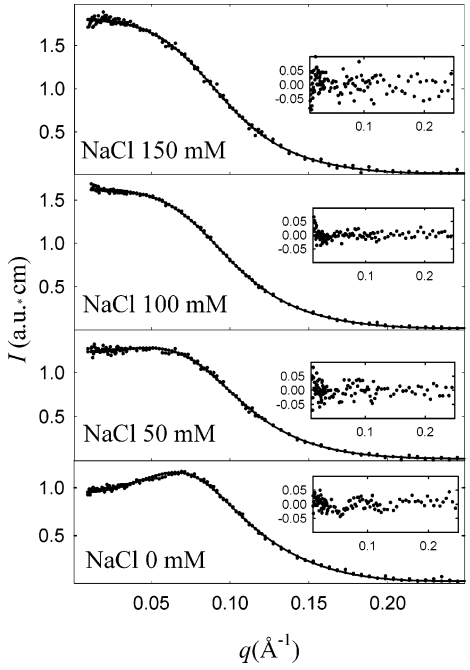

Figure 6. Theoretical fits (solid lines) of the SAXS spectra of Figure 3 up to 0.15 M NaCl concentration on the basis of the EDL interaction model. The residuals are reported in the inset.

dielectric constant of the medium, ϵ_o is the permittivity of the free space, α is the ionization degree, e is the electronic charge, and κ is the Debye Hückel inverse screening length defined as

$$\kappa = \left(\frac{N_A e^2 I 10^3}{k_B T \epsilon \epsilon_o}\right)^{1/2}$$

where $I = 2(cmc + c_{NaCl}) + \alpha(c - cmc)$, and c_{NaCl} is the NaCl molarity. Equations 10 and 11 were used to calculate δ, n, and ϕ_o by assuming $\upsilon = \upsilon_o$ and $\Delta\rho = \Delta\rho_o$. During the minimization procedure d, L, and α were varied. The best fit curves are reported in Figure 6 and the corresponding parameters are listed in Table 1.

As already mentioned, the EDL interaction model is particularly suitable to describe the samples at low ionic strength, where a relevant electric double layer repulsion dominates on the van der Waals attractive component. This means that, among the parameters obtained from the SAXS fits on the basis of the EDL interaction model, those related to the sample without NaCl are particularly reliable. On the basis of the DLVO theory, the double layer repulsion screening, performed by the added electrolyte, can be simply represented by a lowering of κ^{-1} because of the ionic strength increase. With this assumption, a α value of 0.382 (α_J), which is supposed to be constant as a function of the NaCl and NaGDC concentration, was determined in ref 6. If the EDL interaction model is used to approximate the particle interaction potential, the simple decrease of κ^{-1} is sufficient to represent the repulsion screening effect at very low NaCl concentration, where the intermicellar attraction is negligible. On the other hand, by approaching the 0.2 M NaCl concentration the attractive component becomes relevant, and a significant lowering of α is needed to allow the complex interparticle potential to be approximated by the EDL model. For these reasons, α values similar to α_J are obtained only as far as the lowest ionic strengths are considered. However, in the range 0−0.15 M NaCl α decreases very slowly, thus indicating that the effect of the attractive interactions is low and the EDL interaction model keeps its validity. Growing L and constant d values are obtained by increasing the NaCl concentration. These trends point out that the micelles grow by following a rodlike growth mechanism because of the electrolyte addition.

Equations 3−5 are frequently used to interpret photon correlation spectroscopy experiments on solution of rigid rod macromolecules.[28,32] With modification for the effects of electrostatic interaction, they have been applied also to the interpretation of DLS experiments on polyions. In these cases, the effect of electrostatic interactions between charged rodlike particles has been approximated by considering the particles to be rods surrounded by a cylindrical hard core interaction shell. Through a crude extension, the diffusion second virial coefficient for these systems has been calculated by using eqs 3−5 with larger effective length and diameter for the rods. In this paper, the same assumption was employed to model the interaction between the rod shape ionic micelles of NaGDC at low ionic strength. As a first approach, the simplest case of a uniform thickness of the interaction shell was assumed.[28] Hence, by considering this thickness to be equal to $x/2$, $L + x$ and $d + x$ were taken as the effective length and diameter of the particles, respectively.

This hard core (HC) interaction model was successfully used in the literature to interpret DLS measurements on suitable oligonucleotides.[28] However, in our case, before treating the D_{app} data, it was tested as a fitting model of the SAXS patterns already interpreted by assuming the EDL interaction potential. In this frame, a system of hard spheres with an effective diameter δ expressed as

$$\delta = \frac{1}{2}\left\{3(d+x)^2(L+x)\left[\frac{L+x}{d+x} + \frac{1}{2}(3+\pi) + \frac{\pi(d+x)}{4(L+x)}\right]\right\}^{1/3}$$

was used to represent the effective interacting cylinders. On this system, the closed form solution to the Percus Yevick equation was applied to estimate $S(q)$. The same $\upsilon = \upsilon_o$ was considered for all the samples, whereas d, L, and x were varied to fit the experimental spectra. The best fitting curves and the corresponding parameters are reported in Figure 7 and in Table 1, respectively. The $S(q)$ patterns obtained in this interpretation and on the basis of the EDL interaction model are drawn in Figure 8.

As shown in Figure 7, satisfactory agreement between calculated and experimental curves are obtained. Moreover, an inspection of the data reported in Table 1 shows that similar L and d values are obtained by using the HC (L_{HC} and d_{HC}) or the EDL (L_{EDL} and d_{EDL}) interaction model. Despite the similarity of these best fitting parameters, significantly different $S(q)$ patterns are obtained by the two models for the sample without NaCl (Figure 8). However, the agreement between the two $S(q)$ curves rapidly improve by increasing the added electrolyte concentration, and similar $S(q)$ trends are obtained at NaCl concentration $\geq$0.05 M. In view of the already discussed validity of the EDL results, the rough agreement between the two interpretations indicates that the HC model also is suitable to represent the interaction effect in the samples at low ionic strength. This model is particularly reliable if only the samples with some added NaCl are considered.

Numerical solutions of the nonlinear Poisson−Boltzmann equation for polyions with finite length and diameter of 20 Å are reported in the literature.[43] They show that, concerning the electrostatic potential, the polyion can be regarded as effectively infinite in length when $L \geq 2\kappa^{-1}$, with κ^{-1} calculated from the added salt alone. Moreover, they demonstrate that, in a long rodlike polyelectrolyte, the end effect extends to a distance of

TABLE 1: Fitting Parameters of SAXS Spectra at NaCl Concentration ≤0.15 M Obtained by Using the HC Interaction Model (L_{HC}, d_{HC}, x, n_{HC}) and the EDL Interaction Model (L_{EDL}, d_{EDL}, α, n_{EDL}) Together with R_{hHC}, R_{hHCGT} and R_{hEDLGT}[a]

NaCl	L_{HC} (Å)	d_{HC} (Å)	x (Å)	n_{HC}	L_{EDL} (Å)	d_{EDL} (Å)	α	κ^{-1} (Å)	n_{EDL}	R_{hHC} (Å)	R_{hEDLGT} (Å)	R_{hHCGT} (Å)
0.0	37.2(4)	31.6(2)	16.8(1)	32(2)	36.0(4)	31.6(2)	0.322(2)	23.29(7)	31(2)	16(2)		
0.05	45.6(4)	32.0(2)	11.2(1)	40(2)	44.0(8)	32.0(2)	0.298(2)	11.85(1)	39(2)	19(2)	22.2(2)	22.5(2)
0.10	54.8(4)	32.4(2)	7.4(1)	50(2)	51.2(4)	32.8(2)	0.246(2)	9.048(5)	48(2)	21(1)	23.7(2)	24.0(2)
0.15	56.4(8)	33.6(6)	6.0(1)	55(4)	54.0(4)	33.8(2)	0.240(2)	7.537(3)	53(2)	24(1)	24.6(2)	24.9(2)

[a] Esd's are reported in parentheses.

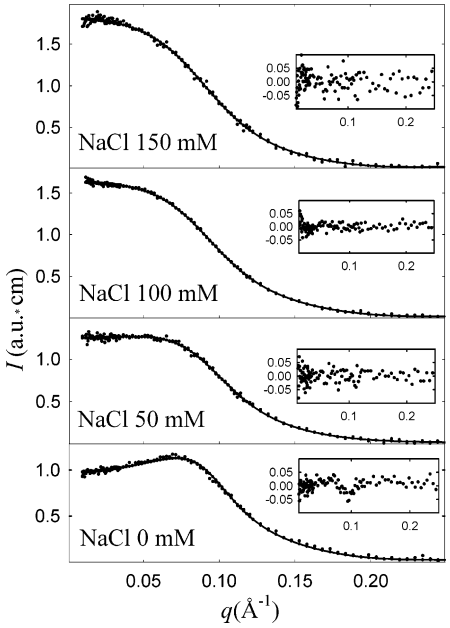

Figure 7. Theoretical fits of the SAXS spectra of Figure 6 on the basis of the HC interaction model. The residuals are reported in the inset.

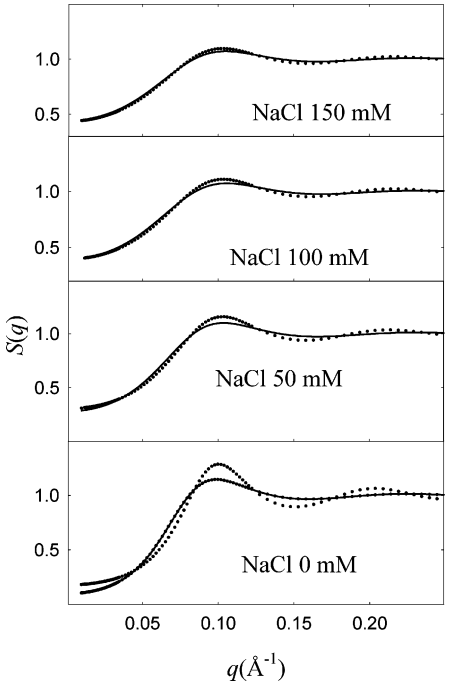

Figure 8. The extracted $S(q)$ curves corresponding to the fits of Figure 6 (full line) and Figure 7 (dotted line).

about $\kappa^{-1}/2$. In the HC model, this distance should be equal to the interaction shell thickness, which means that $x \cong \kappa^{-1}$ is expected for this kind of polyions.[19] Although d values larger than the one supposed for the polyion in the numerical calculations characterize our micelles, x close to κ^{-1} is obtained at all the studied ionic strengths (Table 1). The largest disagreement is observed for the sample without NaCl where, as demonstrated by the $S(q)$ pattern comparison, the HC model is less suitable to describe the particle interaction effect. A decrease of x as a function of the electrolyte concentration testifies the progressive screening of the electrostatic repulsions.

To correlate SAXS and DLS measurements, the D_{app} data were interpreted by using the effective length ($L + x$) and diameter ($d + x$) in eqs 4 and 5, thus obtaining the following expression for the diffusion second virial coefficient

$$\lambda c = \frac{2(d+x)^2(L+x)}{Ld^2}\left[\frac{L+x}{d+x} + \frac{1}{2}(3+\pi) + \frac{\pi}{4}\frac{d+x}{L+x}\right] - \frac{4kT(L+x)^2}{3\pi\eta D_o L d^2}\left[\frac{3(d+x)}{8(L+x)}\right]^{2/3} - 1 \quad (12)$$

Therefore, from the L, d, and x values obtained by fitting the SAXS spectra in the approximation of the HC interaction model, the D_o values were estimated by combining eq 1 and 12 as

$$D_o = \frac{D_{app} + \frac{4kT(L+x)^2}{3\pi\eta L d^2}\left[\frac{3(d+x)}{8(L+x)}\right]^{2/3}\phi}{1 + \left\{\frac{2(d+x)^2(L+x)}{Ld^2}\left[\frac{L+x}{d+x} + \frac{1}{2}(3+\pi) + \frac{\pi}{4}\frac{d+x}{L+x}\right] - 1\right\}\phi}$$

where $\phi = (c - cmc)N_A v_o$ was assumed. The corresponding R_h values (R_{hHC}) were calculated by means of eq 2 and are reported in Table 1.

It has been shown by Eimer and Pecora that the Tirado-Garcia de la Torre treatment of the hydrodynamic of rodlike molecules is self-consistent for length-to-diameter ratios as small as 1.4.[36] Therefore, eq 6 can be used to calculate the translational free diffusion coefficient D_o for the sample containing NaCl by using the L and d values of Table 1. The corresponding hydrodynamic radii can be estimated by means of eq 2. Similar values are obtained from the L and d values derived by the HC (R_{hHCGT}) and the EDL (R_{hEDLGT}) interaction models (Table 1). These radii satisfactorily agree with the R_{hHC} values at the highest NaCl concentration. The agreement gradually get worse at lower ionic strength where the length-to-diameter ratios approach the minimum for the application of eq 6 and the HC interaction model, used in the interpretation of the D_{app} values of Figure 3, progressively loses its reliability.

Conclusions

A comparison between SAXS and DLS measurements indicates that in NaGDC micellar solutions the effect of double layer electric repulsion, that prevails at low ionic strength, is lowered because of the screening effect by increasing the electrolyte concentration. A predominance of the attractive van der Waals potential component is observed at NaCl concentration greater that 0.2 M.

A system of homogeneous monodisperse hard cylinders was used to represent the micelle solution. The decoupling approximation was assumed to estimate the interaction effect on SAXS spectra. The addition of a hard interaction shell of uniform thickness to the cylinders seems to be suitable to model the effect of Coulombic repulsion on $S(q)$ in the range 0.05−0.20 M NaCl concentration. The similarity between the geometrical best fit parameters and the $S(q)$ patterns obtained with this model and those derived by applying the largely accepted Hayter and Penfold method confirms this conclusion. The interaction effect on D_{app} in this model system was evaluated by extending to this case the expression of the diffusion second virial coefficient normally utilized for systems where only the particle excluded-volume contribution is supposed to determine the particle interaction potential. Generally, a satisfactory agreement between the hydrodynamic radii and the geometrical parameters of the SAXS fits is obtained. The larger disagreement is observed for the sample without electrolyte added where the strongest Coulombic repulsion among the micelles is present.

Acknowledgment. This work was sponsored by Italian Ministero dell'Istruzione, dell'Università e della Ricerca (Cofin no. 20020371541).

References and Notes

(1) Weinheimer, R. M.; Evans, D. F.; Cussler, E. L. *J. Colloid Interface Sci*. **1981**, *80*, 357.
(2) Leaist, D. G. *J. Colloid Interface Sci*. **1986**, *111*, 240.
(3) Annunziata, O.; Costantino, L.; D'Errico, G.; Paduano, L.; Vitagliano, V. *J. Colloid Interface Sci*. **1999**, *216*, 8.
(4) Annunziata, O.; Costantino, L.; D'Errico, G.; Paduano, L.; Vitagliano, V. *J. Colloid Interface Sci*. **1999**, *216*, 16.
(5) Paduano, L.; Sartorio, R.; D'Errico, G.; Ortona, O.; Vitagliano, V. *J. Colloid Interface Sci*. **2001**, *239*, 264.
(6) Verwey, E. J. W.; Overbeck, J. Th. G. *Theory of the Stability of Lyophobic Colloids*; Elsevier: New York, 1948.
(7) Small, D. M. In *The Bile Acids*; Nair, P. P., Kritchevsky, D., Eds.; Plenum Press: New York, 1971; Vol. 1, Chapter 8.
(8) Carey, M. C. In *Sterols and Bile Acids*; Danielsson, H., Siøvall, J., Eds.; Elsevier/North-Holland Biomedical Press: Amsterdam, 1985; p 345.
(9) Mazer, N. A.; Carey, M. C.; Kwasnick, R. F.; Benedek, G. B. *Biochemistry* **1979**, *18*, 3064.
(10) Schurtenberger, P.; Mazer, N.; Känzig, W. *J. Phys. Chem*. **1983**, *87*, 308.
(11) Janich, M.; Lange, J.; Graener, H.; Neubert, R. *J. Phys. Chem. B* **1998**, *102*, 5957.
(12) Galantini, L.; Giglio, E.; La Mesa, C.; Pavel, N. V.; Punzo, F. *Langmuir* **2002**, *18*, 2812.
(13) Galantini, L.; Giglio, E.; Pavel, N. V.; Punzo, F. *Langmuir* **2003**, *19*, 1319.
(14) D'Alagni, M.; D'Archivio, A. A.; Galantini, L.; Giglio, E. *Langmuir* **1997**, *13*, 5811.
(15) Bonincontro, A.; Briganti, G.; D'Archivio, A. A.; Galantini, L.; Giglio, E. *J. Phys. Chem. B* **1997**, *101*, 10303.
(16) Bonincontro, A.; D'Archivio, A. A.; Galantini, L.; Giglio, E.; Punzo, F. *J. Phys. Chem. B* **1999**, *103*, 4986.
(17) Corti, M.; Degiorgio, V. *J. Phys. Chem.* **1981**, *85*, 711.
(18) Dorshow, R.; Briggs, J.; Bunton, C. A.; Nicoli, D. F. *J. Phys. Chem.* **1982**, *86*, 2388.
(19) Dorshow, R. B.; Bunton, C. A.; Nicoli, D. F. *J. Phys. Chem*. **1983**, *87*, 1409.
(20) Ortega, F.; Bacaloglu, R.; McKanzie, D. C.; Bunton, C. A.; Nicoli, D. F. *J. Phys. Chem. B* **1990**, *94/2*, 501.
(21) Missel, P. J.; Mazer, N. A.; Benedek, G. B.; Young, C. Y.; Carey, M. C. *J. Phys. Chem.* **1980**, *84*, 1044.
(22) Porte, G.; Appel, J. *J. Phys. Chem*. **1982**, *85*, 2511.
(23) Young, C. Y.; Missel, P. J.; Mazer, N. A.; Benedek, G. B.; Carey, M. C. *J. Phys. Chem*. **1978**, *82*, 1375.
(24) Esposito, G.; Giglio, E.; Pavel, N. V.; Zanobi, A. *J. Phys. Chem*. **1987**, *91*, 356.
(25) Kotlarchyk, M.; Chen, S.-H. *J. Chem. Phys.* **1983**, *79*, 2461.
(26) Hayter, J. B.; Penfold, J. *Mol. Phys.* **1981**, *42*, 109.
(27) Hansen, J.-P.; Hayter, J. B. *Mol. Phys.* **1982**, *46*, 651.
(28) Liu, H.; Skibinska, L.; Gapinski, J.; Patkowski, A.; Fischer, E. W.; Pecora, R. *J. Chem. Phys*. **1998**, *109*, 7556.
(29) Siegert, A. J. F. *MIT Rad. Lab. Rep. No*. **1943**, 465.
(30) Koppel, D. E. *J. Chem. Phys*. **1972**, *57*, 4814.
(31) Pusey, P. N.; Tough, R. J. A. In *Dynamic Light Scattering*; Pecora, R., Ed.; Plenum: New York, 1985; Chapter 4.
(32) Tracy, M. A.; Pecora, R. *Macromolecules* **1992**, *25*, 337.
(33) Ishihara, A. *J. Chem. Phys.* **1950**, *18*, 1446.
(34) Peterson, J. *J. Chem. Phys.* **1964**, *40*, 2680.
(35) Garcia de la Torre, J.; Lopez Martinez, M. C.; Tirado, M. M. *Biopolymers* **1984**, *23*, 611.
(36) Eimer, W.; Pecora, R. *J. Chem. Phys.* **1991**, *94*, 2324.
(37) Galantini, L.; Pavel, N. V. *J. Chem. Phys.* **2003**, *118*, 2865.
(38) Bendedouch, D.; Chen, S.-H.; Koehler, W. C. *J. Phys. Chem*. **1983**, *87*, 2621.
(39) Bendedouch, D.; Chen, S.-H. *J. Phys. Chem.* **1984**, *88*, 648.
(40) Long, M. A.; Kaler, E. W.; Lee, S. P.; Wignall, G. D. *J. Phys. Chem.* **1994**, *98*, 4402.
(41) Stabinger, H.; Kratky, O. *Makromol. Chem.* **1978**, *179*, 1655.
(42) Glatter O. *J. Appl. Crystallogr*. **1974**, *7*, 147.
(43) Katoh, T.; Ohtsuki, T. *J. Polym. Sci. Polym. Phys. Ed.* **1982**, *20*, 2167.